MDO Assignment

MDF implementation conceptual design phase Boeing 737-600
Full Report

Group 31:

[redacted] & Ribhav Khanduja (5337887)

Febuary 2022

Contents

1 Part 1

1.1 Introduction

An Multiple Discipline Feasible (MDF) implementation of the conceptual design phase of the Boeing 737-600 wing is set up. It is desired to minimize the fuel weight while keeping all design variables within acceptable bounds.

Initially, the wing is parametrized. Secondly, the mathematical problem statement is given. Then the design vector and constraints are given, as well as three tables that contain all relevant constants, design variables and other variables. Finally, an XDSM table showing the information and process flow through different disciplines and the optimiser is given.

In the table of constants, all constants relevant to the design optimization are given, including their symbols, values and units. The table with design variables gives all design variables, as well as their symbols, lower and upper bounds and units. The table with all other variables shows all variables that may result from the calculations of the four disciplines, or can be calculated using the design variables.

1.2 Parametrization

The wing geometry is parametrized in figure 1. The chord lengths (root and tip), twist angles (kink and tip), sweep angles (inner and outer trapezoid), and outer span are defined as design variables. The x, y and z coordinates of the wing root, kink and wing tip section are calculated from the previously defined variables, and the chordwise locations of the front- and rear spars along the wingspan are fixed.

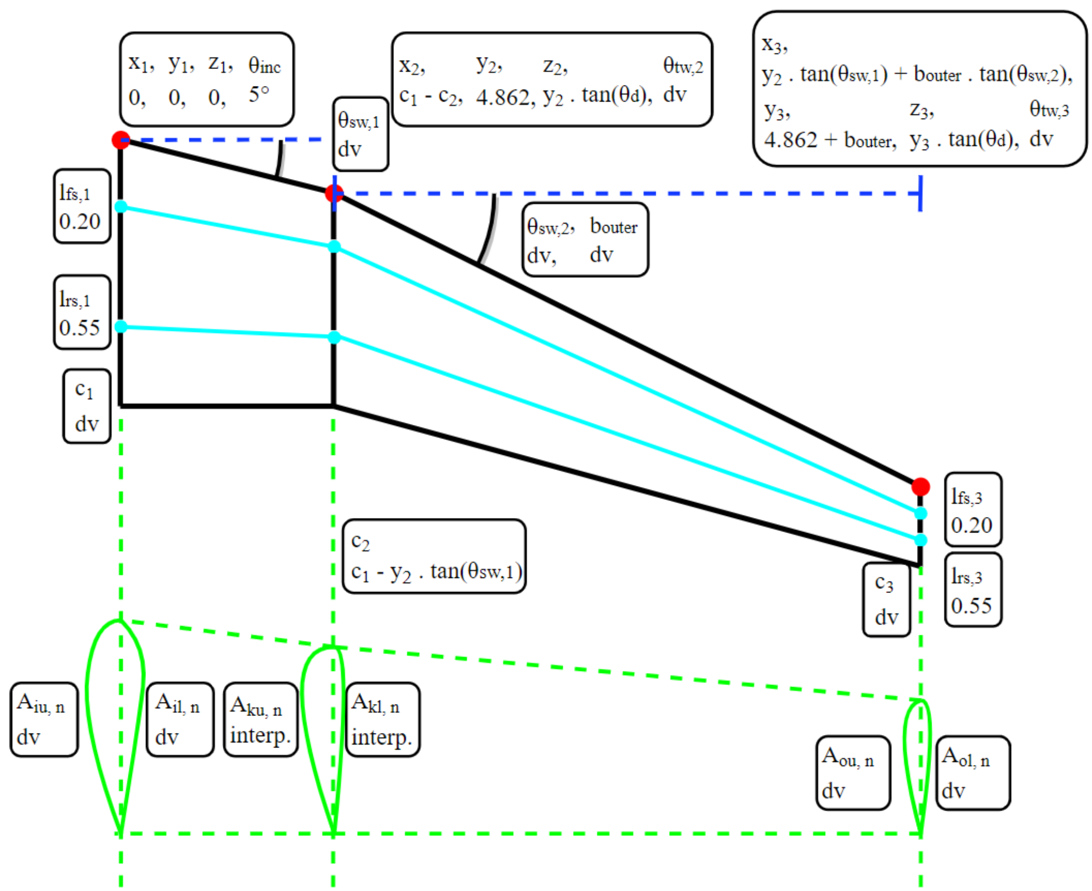

Figure 1: Parametrization of the wing. Note: dv stands for design variable and interp. stands for interpolated variable.

The reason these design variables were chosen to be the design variables is because they allow for a better bounding of the design space than using direct x- and y-coordinates as design variables. Attempting an optimisation with the coordinates as the design variables led to a very unfeasible shape for the wing. The incidence angle is set to a static value of 5° because Q3D calculates the angle of attack to be $\theta_{inc}+\theta_{tw}$, which can be expressed in terms of θ_{inc} only, avoiding redundancy.

The upper and lower bounds for the geometric design variables were chosen such that they were 15% higher and lower than the reference values. These bounds were chosen because they allowed for reasonable variation in the geometry of the wing, for e.g., the sweep angles can vary anywhere from 21.25 to 28.75°. A higher difference in the inner and outer sweep angles may lead to structural weaknesses in the wing as the front and rear spars are fixed at 0.2 and 0.55 chordwise locations respectively, and the spars will also need to bend to accommodate for the change in sweep. The upper bound of b_{outer} follows from the maximum wingspan of this class of aircraft, which is said to be 36 meters. At an already high initial wingspan of 34.32 meters, it was decided to limit the upper bound of b_{outer} to 100% to leave room for clearance and/or winglets to be installed.

The upper and lower bounds for the airfoil design variables (Bernstein coefficients) were chosen to allow a 30% increase or decrease from the reference values. Increasing these bounds in previous optimisations have shown very drastic and unrealistic changes in the airfoil shapes which also had severe consequences on the optimisation itself. As the aerodynamic discipline (Viscous Analysis in Q3D) is very sensitive to changes in the airfoil shapes, higher bounds led it to not converge in some function evaluations.

The x, y and z coordinates of the leading edge of the root chord are set to 0, 0 and 0 respectively. Some coordinates are expressed in terms of constants and other variables. These coordinates are explained below:

- x_2: To satisfy the no sweep at the trailing edge requirement at the kink, $x_2 = c_1 - c_2$
- c_2: The chord at the kink can also be defined by the chord at the root and the first sweep angle, $c_2 = c_1 - y_2 \ . \ tan(\theta_{sw,1})$
- y_2: The spanwise distance of the kink with respect to the fuselage centerline is found to be 4.862 meters for the reference aircraft and remains constant during the optimalisation process.
- z_2 & z_3: The z-coordinates can be expressed in terms of the dihedral angle and their respective y-coordinates

Other wing properties, such as the surface area, aspect ratio, taper ratio and the volume of the wing (fuel tank), etc., can be expressed in terms of the above stated design variables. Note, while figure 1 shows the Bernstein coefficients being interpolated at the kink from the root and tip airfoils, in actuality, the airfoil coordinates are directly interpolated for simplicity. A total of 7 Bernstein coefficients were used for each half of an airfoil, making it a 6th order CST parametrization. The volume of the fuel tank was calculated by averaging the area of 2 consecutive airfoils (in between the front and rear spars, and from the root to kink, then the kink to 85% span), and then multiplying it by the orthogonal distance between said consecutive airfoils and a safety margin of 0.93.

1.3 Problem statement

The objective is to minimize the maximum take-off weight of the Boeing 737-600 by finding the optimum values of the design variables, while keeping everything within bounds. The mathematical problem statement is given below:

Minimize

$$W_{fuel}(\bar{q}) = \left[1 - 0.938 \cdot \frac{W_{end-cr}}{W_{start-cr}}(\bar{q})\right] \cdot W_{TO\_max}(\bar{q}) \tag{1}$$

Where

$$W_{TO\_max}(\bar{q}) = \frac{(W_{AW} + W_{wing}(\bar{q}))}{1 - (0.938 \cdot \frac{W_{end-cr}}{W_{start-cr}}(\bar{q}))} \tag{2}$$

And

$$\frac{W_{start-cr}}{W_{end-cr}}(\bar{q}) = e^{R \cdot \frac{C_T}{v_{cruise}} \cdot \frac{D}{L}(\bar{q})} \tag{3}$$

With respect to:

$$\begin{gathered} \theta_{sw,1} \\ \theta_{sw,2} \\ c_1, c_3 \\ \mathrm{b}_{outer} \\ \theta_{tw,2}, \theta_{tw,3} \\ \mathbf{A}_{i,u} \\ \mathbf{A}_{i,l} \\ \mathbf{A}_{o,u} \\ \mathbf{A}_{o,l} \end{gathered}$$

Subject to:

$$\frac{W_{fuel}(\bar{q}) - W_{tank}(\bar{q})}{W_{tank}(\bar{q})} \leq 0 : \tag{4}$$

With:

$$W_{tank}(\bar{q}) = V_{tank}(\bar{q}) \cdot 9.81 \cdot \rho_f \tag{5}$$

And:

$$V_{tank}(\bar{q}) = 0.93 \cdot \left[\frac{S_{af_1}(\bar{q}) + S_{af_2}(\bar{q})}{2} \cdot y_2 + \frac{S_{af_2}(\bar{q}) + S_{af_{85}}(\bar{q})}{2} \cdot (0.85 y_3(\bar{q}) - y_2)\right] \tag{6}$$

And

$$\frac{W_{TO\_max}(\bar{q})}{S(\bar{q})} - \frac{W_{TO\_max,ref}}{S_{ref}} \leq 0 : \tag{7}$$

With:

$$S(\bar{q}) = \sum_{i=1}^{2} \frac{c_i(\bar{q}) + c_{i+1}(\bar{q})}{2} \cdot (y_{i+1}(\bar{q}) - y_i(\bar{q})) \tag{8}$$

1.4 Initialisation

For the initialisation of the reference aircraft, the value of the maximum take off mass was fixed at 65090 kg in all disciplines, and the lift to drag ratio was also fixed at 16 in the aerodynamic discipline. With these constraints, the fuel and wing weight were allowed to converge in the MDA coordinator, which gave the reference values shown in table 7. The slight deviation in the objective function value and total lift to drag ratio is due to the minimum error allowed for the convergence of the disciplines. This convergence was also used to determine the Drag force and Weight of the A-W group of the aircraft, which were then fixed for the optimisation.

1.5 Tables

Constants	**Symbols**	**Values**	**Units**
Cruise flight speed	v_{cruise}	231.5	m/s
Cruise Mach number	M_{cruise}	0.7846	[-]
Critical flight speed	v_{crit}	247.86	m/s
Critical Mach number	M_{crit}	0.84	[-]
Cruise & Critical altitude	h_{cruise}	11887.2	m
Cruise & Critical air density	ρ_a	0.3164	kg/m^3
Drag of A-W group	D_{AW}	10535	N
Dihedral angle	θ_d	6	[-] (°)
Incidence angle	θ_i	5	[-] (°)
Reference lift to drag ratio	$C_l/C_{d,ref}$ (L/D_{ref})	16	[-]
Load factor for critical conditions	n	2.5	[-]
Initialised A-W group weight	$W_{AW,init}$	369040	N
Non-dimensional chordwise locations of the front spar	$\mathbf{l}_{fs,n}\ \forall_{n=(1,2,3)}$	0.20	[-]
Non-dimensional chordwise locations of the rear spar	$\mathbf{l}_{rs,n}\ \forall_{n=(1,2,3)}$	0.55	[-]
Number of sections to define the wing spanwise cross section	N_p	3	[-]
Number of sections to define airfoils	N_a	3	[-]
Spanwise location of inboard airfoil	$y/(b/2)_{in}$	0	[-]
Spanwise location of outboard airfoil	$y/(b/2)_{out}$	1	[-]
Inboard airfoil name	af_1	whitcomb(14t/c).dat	[-]
Kink airfoil name	af_2	whitcombinterp.dat	[-]
Outboard airfoil name	af_3	whitcomb(8t/c).dat	[-]
Spanwise start of fuel tank	$y/(b/2)_{stf}$	0	[-]
Spanwise end of fuel tank	$y/(b/2)_{enf}$	0.85	[-]
Number of engines per half wing	$N_{engines}$	1	[-]
Engine mass	M_{eng}	2385	kg
Young's modulus aluminum	Y	$70 \cdot 10^9$	N/m^2
Material density	ρ_m	2800	kg/m^3
Tensile yield stress	σ_t	$295 \cdot 10^9$	N/m^2
Compressive yield stress	σ_c	$295 \cdot 10^9$	N/m^2
Stiffened panel efficiency factor	F	0.95	[-]
Rib pitch	P_R	0.5	m
Specific fuel consumption	C_T	0.00018639	N/Ns
Tank approximation factor	f_{tank}	0.93	[-]
Fuel density	ρ_f	817.15	kg/m^3
Flight range	R	5909	km

Table 1: Table of constant values that are used in the MDF MDO setup, including values and units

Variables	Symbols	Units
Cruise average chord length Reynolds number	Re_c	[-]
Surface area of the wing	S	m^2
Surface area of airfoil n where n = 1, 2, 3, 85 (root, kink, tip, 85% span)	S_{af_n}	m^2
Total wing span	b	m
Non dimensional spanwise location of the kink and engine	l_{kink}	[-]
Wing total lift coefficient	C_l	[-]
Wing total drag coefficient	C_d	[-]
Main airframe total drag coefficient	$C_{d,A-W}$	[-]
Start cruise weight	$W_{start-cr}$	N
End cruise weight	W_{end-cr}	N
Volume of fuel tank	V_{tank}	m^3
Fuel weight	W_{fuel}	N
Wing weight	W_{wing}	N

Table 2: Table of variables that are output from the IDF MDO setup, including their symbols and units

Design Variables	Symbols	Initial values	Lower Bounds	Upper Bounds	Units
Sweep angle of leading edge of inner wing	$\theta_{sw,1}$	25	21.25	28.75	[-] (°)
Sweep angle of leading edge of outer wing	$\theta_{sw,2}$	25	21.25	28.75	[-] (°)
Chord lengths	$\mathbf{c}_n\ \forall_{n=(1,3)}$	7.88, 1.24	6.70, 1.06	9.06, 1.44	m
Span outer trapezoid	b$_{outer}$	12.298	10.45	14.14	m
twist angles at each spanwise cross section	$\boldsymbol{\theta}_{tw,n}\ \forall_{n=(2,3)}$	-5, -7	-4.25, -5.95	-5.75, -8.05	[-] (°)
Upper CST coefficients Root section	$\mathbf{A}_{i,u,n}\ \forall_{n=(1,\ldots,7)}$	0.250417 0.077947 0.299518 0.053087 0.292163 0.221428 0.435421	70%	130%	[-]
Lower CST coefficients Root section	$\mathbf{A}_{i,l,n}\ \forall_{n=(1,\ldots,7)}$	-0.248007 -0.117146 -0.259831 -0.007221 -0.572253 0.295035 0.266428	70%	130%	[-]
Upper CST coefficients Tip section	$\mathbf{A}_{o,u,n}\ \forall_{n=(1,\ldots,7)}$	0.143107 0.044483 0.171302 0.030098 0.167200 0.126350 0.248897	70%	130%	[-]
Lower CST coefficients Tip section	$\mathbf{A}_{o,l,n}\ \forall_{n=(1,\ldots,7)}$	-0.141727 -0.066888 -0.148618 -0.003892 -0.327246 0.168758 0.152176	70%	130%	[-]

Table 3: Table of design variables that are used in the MDF MDO setup, including symbols, upper bounds, lower bounds and units

2 XDSM

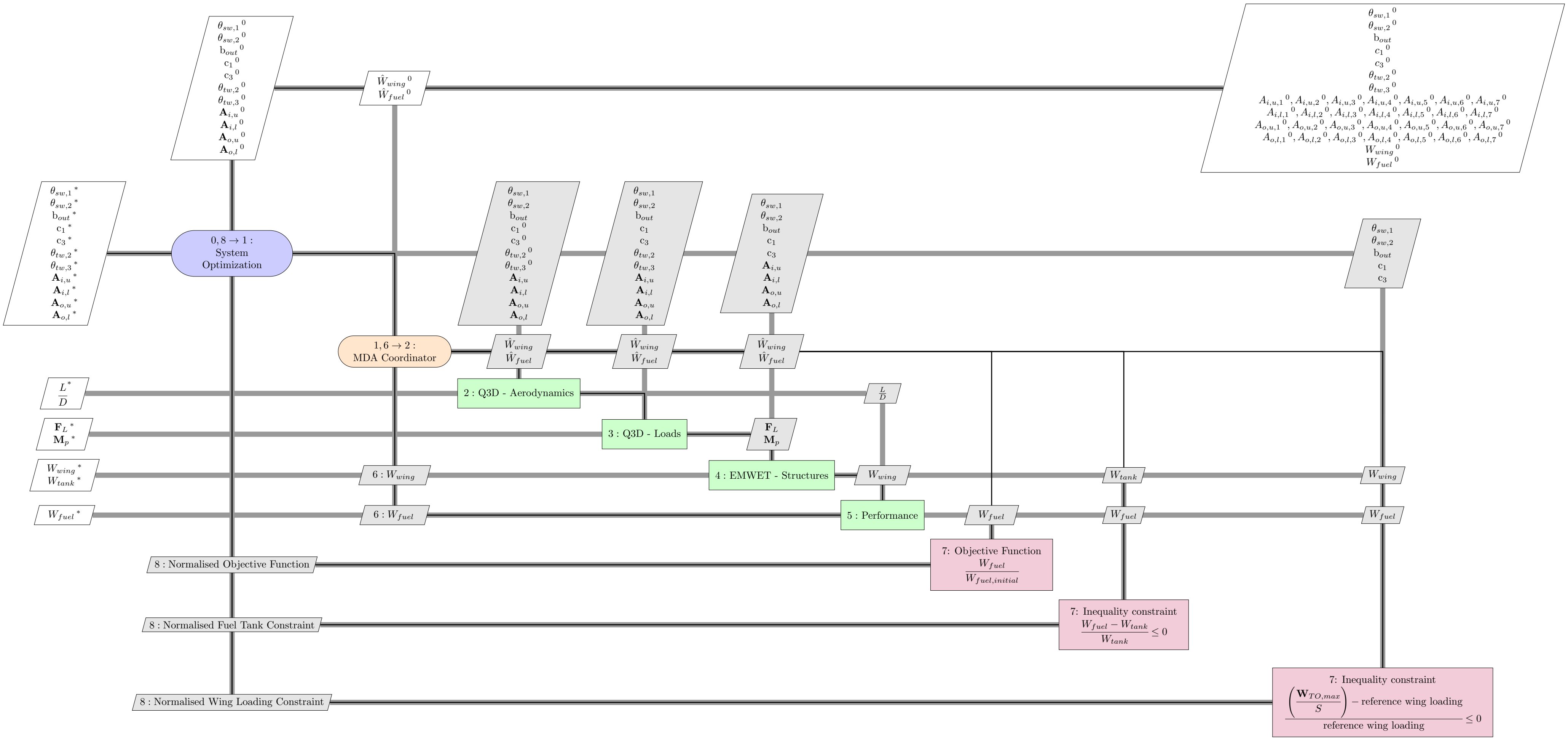
0, 8 → 1 : System Optimization
1, 6 → 2 : MDA Coordinator
2 : Q3D - Aerodynamics
3 : Q3D - Loads
4 : EMWET - Structures
5 : Performance
7: Objective Function $\frac{W_{fuel}}{W_{fuel,initial}}$
7: Inequality constraint $\frac{W_{fuel} - W_{tank}}{W_{tank}} \leq 0$
7: Inequality constraint $\frac{\left(\frac{\mathbf{W}_{TO,max}}{S}\right) - \text{reference wing loading}}{\text{reference wing loading}} \leq 0$
8 : Normalised Objective Function
8 : Normalised Fuel Tank Constraint
8 : Normalised Wing Loading Constraint
6 : W_{wing}
6 : W_{fuel}
$\hat{W}_{wing}^0$, $\hat{W}_{fuel}^0$
$\hat{W}_{wing}$, $\hat{W}_{fuel}$
$\frac{L}{D}$
$\frac{L}{D}^*$
$\mathbf{F}_L^*$, $\mathbf{M}_p^*$
$\mathbf{F}_L$, $\mathbf{M}_p$
W_{wing}^*, W_{tank}^*
W_{fuel}^*
W_{wing}
W_{tank}
W_{fuel}
$\theta_{sw,1}^0$, $\theta_{sw,2}^0$, b_{out}^0, c_1^0, c_3^0, $\theta_{tw,2}^0$, $\theta_{tw,3}^0$, $\mathbf{A}_{i,u}^0$, $\mathbf{A}_{i,l}^0$, $\mathbf{A}_{o,u}^0$, $\mathbf{A}_{o,l}^0$
$\theta_{sw,1}^*$, $\theta_{sw,2}^*$, b_{out}^*, c_1^*, c_3^*, $\theta_{tw,2}^*$, $\theta_{tw,3}^*$, $\mathbf{A}_{i,u}^*$, $\mathbf{A}_{i,l}^*$, $\mathbf{A}_{o,u}^*$, $\mathbf{A}_{o,l}^*$
$\theta_{sw,1}$, $\theta_{sw,2}$, b_{out}, c_1^0, c_3^0, $\theta_{tw,2}^0$, $\theta_{tw,3}^0$, $\mathbf{A}_{i,u}$, $\mathbf{A}_{i,l}$, $\mathbf{A}_{o,u}$, $\mathbf{A}_{o,l}$
$\theta_{sw,1}$, $\theta_{sw,2}$, b_{out}, c_1, c_3, $\theta_{tw,2}$, $\theta_{tw,3}$, $\mathbf{A}_{i,u}$, $\mathbf{A}_{i,l}$, $\mathbf{A}_{o,u}$, $\mathbf{A}_{o,l}$
$\theta_{sw,1}$, $\theta_{sw,2}$, b_{out}, c_1, c_3, $\mathbf{A}_{i,u}$, $\mathbf{A}_{i,l}$, $\mathbf{A}_{o,u}$, $\mathbf{A}_{o,l}$
$\theta_{sw,1}$, $\theta_{sw,2}$, b_{out}, c_1, c_3
$\theta_{sw,1}^0$, $\theta_{sw,2}^0$, b_{out}, c_1^0, c_3^0, $\theta_{tw,2}^0$, $\theta_{tw,3}^0$
$A_{i,u,1}^0, A_{i,u,2}^0, A_{i,u,3}^0, A_{i,u,4}^0, A_{i,u,5}^0, A_{i,u,6}^0, A_{i,u,7}^0$
$A_{i,l,1}^0, A_{i,l,2}^0, A_{i,l,3}^0, A_{i,l,4}^0, A_{i,l,5}^0, A_{i,l,6}^0, A_{i,l,7}^0$
$A_{o,u,1}^0, A_{o,u,2}^0, A_{o,u,3}^0, A_{o,u,4}^0, A_{o,u,5}^0, A_{o,u,6}^0, A_{o,u,7}^0$
$A_{o,l,1}^0, A_{o,l,2}^0, A_{o,l,3}^0, A_{o,l,4}^0, A_{o,l,5}^0, A_{o,l,6}^0, A_{o,l,7}^0$
W_{wing}^0, W_{fuel}^0

3 Part 2

3.1 Termination criteria

Table 4 shows the termination criteria of the solver.

Name	**Value**
options.Display	iter-detailed
options.Algorithm	sqp
options.FunValCheck	off
options.DiffMinChange	0.05
options.DiffMaxChange	0.1
options.TolCon	1e-6
options.TolFun	1e-6
options.TolX	1e-12
options.PlotFcns	@optimplotfval @optimplotx @optimplotfirstorderopt @optimplotstepsize @optimplotconstrviolation @optimplotfunccount
options.MaxIter	150
options.ScaleProblem	false
options.FiniteDifferenceType	central

Table 4: Termination criteria

3.2 Termination message

Figure 2 shows the termination messages.

```
Optimization stopped because the relative changes in all elements of x are
less than options.StepTolerance = 1.000000e-12, and the relative maximum constraint
violation, 0.000000e+00, is less than options.ConstraintTolerance = 1.000000e-06.

time_taken =
   4.3974e+04
```

Figure 2: Termination message

The full termination message reads as follows:

Local minimum possible. Constraints satisfied. fmincon stopped because the size of the current step is less than the value of the step size tolerance and constraints are satisfied to within the value of the constraint tolerance. < stopping criteria details > Optimization stopped because the relative changes in all elements of x are less than options.StepTolerance = 1.000000e-12, and the relative maximum constraint violation, 0.000000e+00, is less than options.ConstraintTolerance = 1.000000e-06.

3.3 Results

Table 5 displays the time needed to reach convergence, as well as the number of iterations and function evaluations. Lastly, table 5 shows the average time required to finish one iteration.

Table 6 compares the initial and optimized values of the design variables. As can be seen from the last column, many of the design variables have reached an upper or lower bound.

Table 7 compares the values of relevant parameters between the reference and the optimized wing. The converged objective value is 0.90281, which means a reduction of 9.72% in the fuel consumption for the given range is achieved through the optimization procedure.

Name	**Value**
Time needed to converge to optimum (or reach termination)	43974 seconds
Number of iterations and objective function evaluations required	Iterations: 26 Function evaluations: 1089
Average time per iteration	1691 seconds

Table 5: Runtime information

Design Variable	**Symbol**	**Initial value**	**Optimized value**	**Nondimensionalized value**
Sweep angle of leading edge of inner wing	$\theta_{sw,1}$	25	21.25	0.850
Sweep angle of leading edge of outer wing	$\theta_{sw,2}$	25	28.75	1.150
Chord lengths	$\mathbf{c}_n\ \forall_{n=(1,3)}$	7.88, 1.24	7.55, 1.09	0.958, 0.878
Span outer trapezoid	b_{outer}	12.298	12.298	1.00
twist angles at each spanwise cross section	$\boldsymbol{\theta}_{tw,n}\ \forall_{n=(2,3)}$	-5, -7	-4.250, -5.950	0.850, 0.850
Upper CST coefficients Root section	$A_{i,u,n}\ \forall_{n=(1,\ldots,7)}$	0.250417 0.077947 0.299518 0.053087 0.292163 0.221428 0.435421	0.175292 0.101331 0.209663 0.064978 0.257619 0.156310 0.304795	0.700 1.300 0.700 1.224 0.882 0.706 0.700
Lower CST coefficients Root section	$A_{i,l,n}\ \forall_{n=(1,\ldots,7)}$	-0.248007 -0.117146 -0.259831 -0.007221 -0.572253 0.295035 0.266428	-0.173633 -0.152204 -0.334361 -0.006669 -0.543111 0.206524 0.186500	0.700 1.299 1.286 0.923 0.949 0.700 0.700
Upper CST coefficients Tip section	$A_{o,u,n}\ \forall_{n=(1,\ldots,7)}$	0.143107 0.044483 0.171302 0.030098 0.167200 0.126350 0.248897	0.100175 0.047256 0.222692 0.031830 0.217360 0.163013 0.323566	0.700 1.062 1.300 1.057 1.299 1.290 1.300
Lower CST coefficients Tip section	$A_{o,l,n}\ \forall_{n=(1,\ldots,7)}$	-0.141727 -0.066888 -0.148618 -0.003892 -0.327246 0.168758 0.152176	-0.148812 -0.069456 -0.157203 -0.003723 -0.229074 0.219377 0.197828	1.049 1.038 1.057 0.956 0.700 1.299 1.299

Table 6: Comparison value of design variables between initial and optimized wings

<table>
<tr><th>Name</th><th colspan="6">Value reference design</th><th colspan="6">Value optimized design</th></tr>
<tr><td>Objective Function Value</td><td colspan="6">1.00001</td><td colspan="6">0.90281</td></tr>
<tr><td>Wing Loading Constraint Value</td><td colspan="6">0.00</td><td colspan="6">-4.75327e-5</td></tr>
<tr><td>Fuel Tank Constraint Value</td><td colspan="6">0.00</td><td colspan="6">-0.332817</td></tr>
<tr><td>Fuel Weight $[N]$</td><td colspan="6">193662</td><td colspan="6">174847</td></tr>
<tr><td>Wing Structure Weight $[N]$</td><td colspan="6">75834.6</td><td colspan="6">83759.3</td></tr>
<tr><td>Maximum Take-Off Weight $[N]$</td><td colspan="6">638537</td><td colspan="6">627646</td></tr>
<tr><td>Fuel Volume $[m^3]$</td><td colspan="6">24.1587</td><td colspan="6">21.8116</td></tr>
<tr><td>Fuel Tank Volume $[m^3]$</td><td colspan="6">34.1783</td><td colspan="6">32.6904</td></tr>
<tr><td>C_L $[-]$</td><td colspan="6">0.419440</td><td colspan="6">0.426930</td></tr>
<tr><td>$C_D, Wing$ $[-]$</td><td colspan="6">0.017924</td><td colspan="6">0.015118</td></tr>
<tr><td>Total Lift to Drag Ratio $[-]$</td><td colspan="6">16.00026</td><td colspan="6">18.12481</td></tr>
<tr><td>Aircraft Body Drag $[N]$</td><td colspan="6">10535</td><td colspan="6">10535</td></tr>
<tr><td>$C_{D,A-W}$ $[-]$</td><td colspan="6">0.041453</td><td colspan="6">0.042185</td></tr>
<tr><td>Aircraft Body and Payload Weight $[N]$</td><td colspan="6">369040</td><td colspan="6">369040</td></tr>
<tr><td>Total Wing Surface Area $[m^2]$</td><td colspan="6">149.878</td><td colspan="6">147.279</td></tr>
<tr><td>Wing Loading $[N/m^2]$</td><td colspan="6">4260.38</td><td colspan="6">4261.60</td></tr>
<tr><td>Sweep Angles (Inner, Outer) $[°]$</td><td colspan="3">25</td><td colspan="3">25</td><td colspan="3">21.25</td><td colspan="3">28.75</td></tr>
<tr><td>Chords (Inner, Kink, Outer) $[m]$</td><td colspan="2">7.8800</td><td colspan="2">5.6128</td><td colspan="2">1.2400</td><td colspan="2">7.5533</td><td colspan="2">5.6625</td><td colspan="2">1.0885</td></tr>
<tr><td>Total Wingspan $[m]$</td><td colspan="6">34.3200</td><td colspan="6">34.3200</td></tr>
<tr><td>Inner Wingspan (Root to Kink) $[m]$</td><td colspan="6">4.862</td><td colspan="6">4.862</td></tr>
<tr><td>Outer Wingspan (Kink to Tip) $[m]$</td><td colspan="6">12.2980</td><td colspan="6">12.2980</td></tr>
<tr><td>Wing Aspect Ratio $[-]$</td><td colspan="6">7.8588</td><td colspan="6">7.9975</td></tr>
<tr><td>Twist Angles (Kink, Tip) $[°]$</td><td colspan="3">-5.00</td><td colspan="3">-7.00</td><td colspan="3">-4.25</td><td colspan="3">-5.95</td></tr>
</table>

Table 7: Numerical parameter comparison of initial and optimized wings

Figure 3 shows the convergence history of the objective function and its values at each iteration. Initially, the objective value reduces quickly, after which it approaches its termination value of 0.90281 while meeting the inequality constraint requirements.

Figure 4 shows the convergence history of the inequality constraints and their values at each iteration. Initially, the inequality constraints are higher than 1. The fuel tank constraint stays well below 1 for the rest of the optimization run because the wing fuel tank was initially designed to be able to hold 26000kg of fuel. For the optimized design, too, the maximum amount of fuel the tank is able to hold is higher than the amount of fuel required for the flight of 5909km. The wing loading constraint was above 0 for most of the optimization run, but the optimizer was able to push the value below 1e-6 (0.00) before terminating.

Figure 5 shows the spanwise lift distribution for the initial and optimized wings at both the design conditions and critical conditions. For the optimized wing design, the lift distributions more closely resemble an elliptical lift distribution which increases the Oswald efficiency factor, which in turn reduces the induced drag experienced by the wing. A reduction in induced drag in turn increases the $\frac{L}{D}$ ratio which reduces the required fuel. Reducing the objective function value, therefore, has been (in part) achieved by improving the spanwise lift distribution of the wing.

Figure 6 shows the spanwise drag coefficients (separate induced and profile+wave drag) for both the initial and optimized wings at the design conditions. For the optimized wing, the profile and wave drag term has been decreased in absolute sense. The induced drag coefficient has decreased near the root airfoil and increased towards the tip. The surface area near the root is much larger than near the tip. It is therefore beneficial to decrease the drag coefficient near the root at the expense of increasing the drag coefficient near the tip because the total $\frac{L}{D}$ ratio can be increased this way.

Figure 7 shows the initial and optimized planform viewed from above. In table 7, it can be seen that the chord lengths have been reduced. One method to increase the efficiency is to increase the aspect ratio (AR). Increasing the AR can be achieved by increasing the wing span or by decreasing the surface area by decreasing the chord lengths. Since the wing span had an upper bound of 100% due to regulatory limitations, the optimizer increased the AR by reducing the chord lengths. By increasing the outer sweep, the relative span width of the wing can be increased while maintaining the absolute maximum span width of 17.16m.

Figures 8 and 9 show the initial and optimized root and tip airfoils for chord length = 1. For the root airfoil, the leading edge has become sharper which decreases a local suction peak. Perhaps a reduction in the leading edge suction peak was beneficial to align the chordwise isobars over the whole planform, though this is outside of the scope of this assignment. The tip airfoil looks like the optimizer tried to increase the twist angle by lifting the trailing edge up slightly.

Figures 10 and 11 show the isometric view of the initial and final wing shapes. All geometric changes can be viewed in 3D, which allows the reader to see the real full 3D shape of the initial and optimized wings. It can be clearly observed that the inboard leading edge radius has decreased and the increased sweep has become clearly visible as one of the most pronounced geometric features.

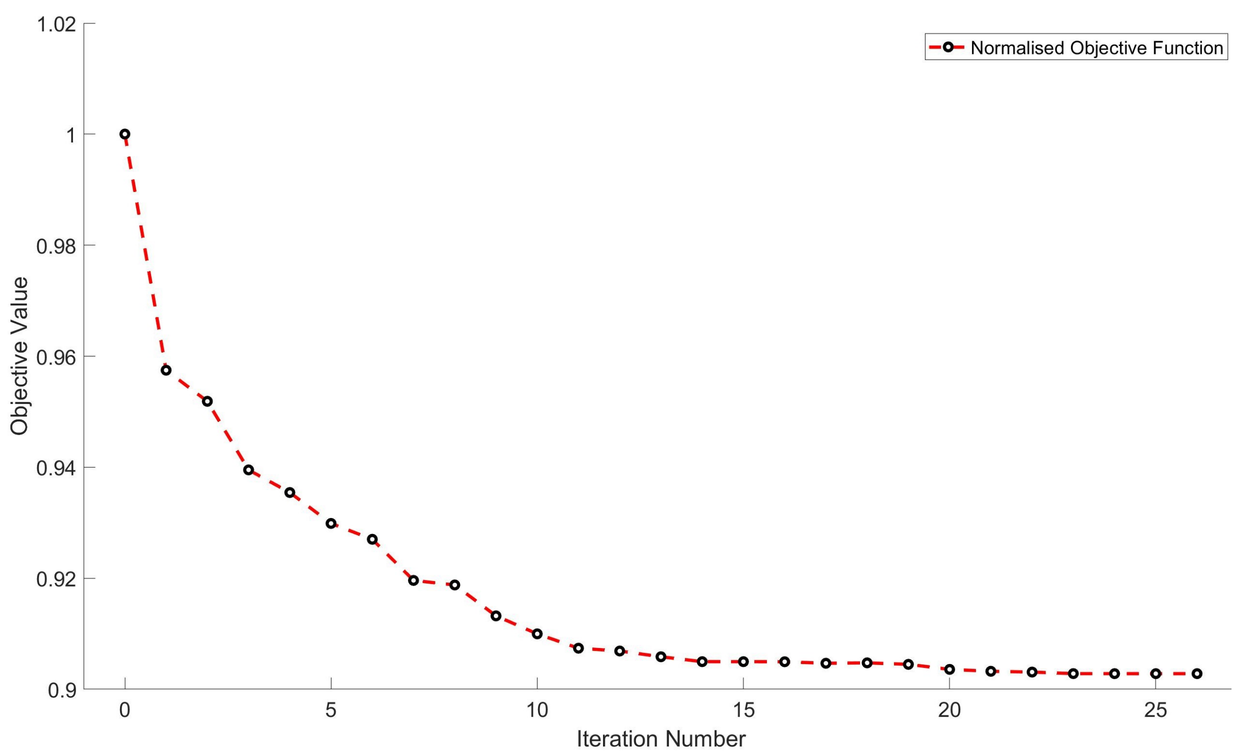

Figure 3: History of objective function value at each iteration

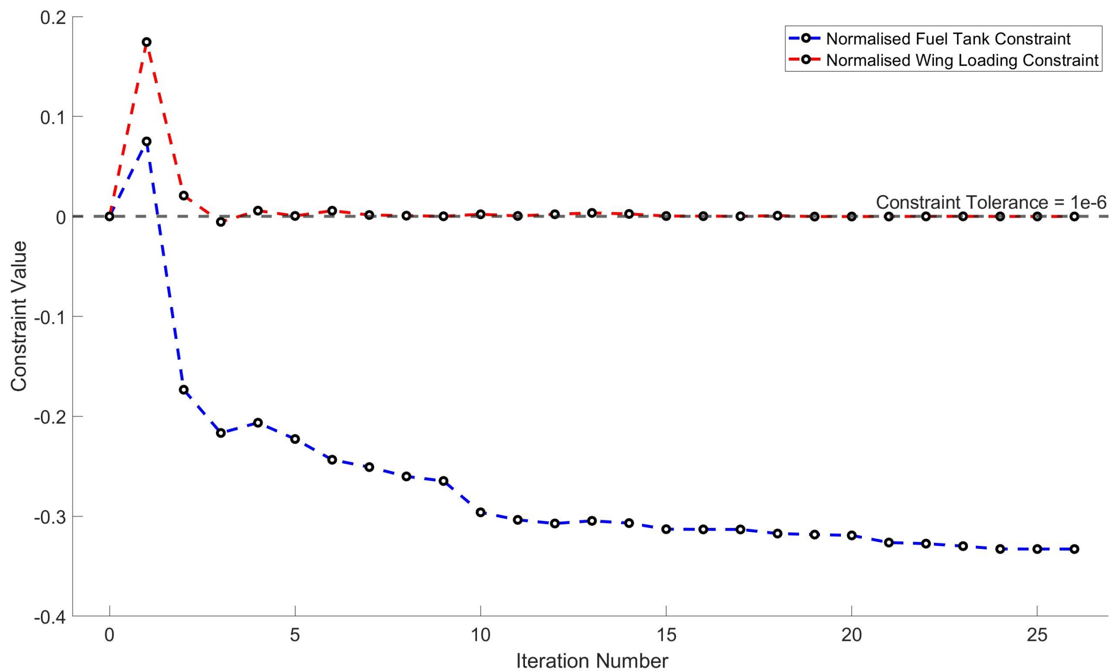

Figure 4: History of inequality constraint values at each iteration

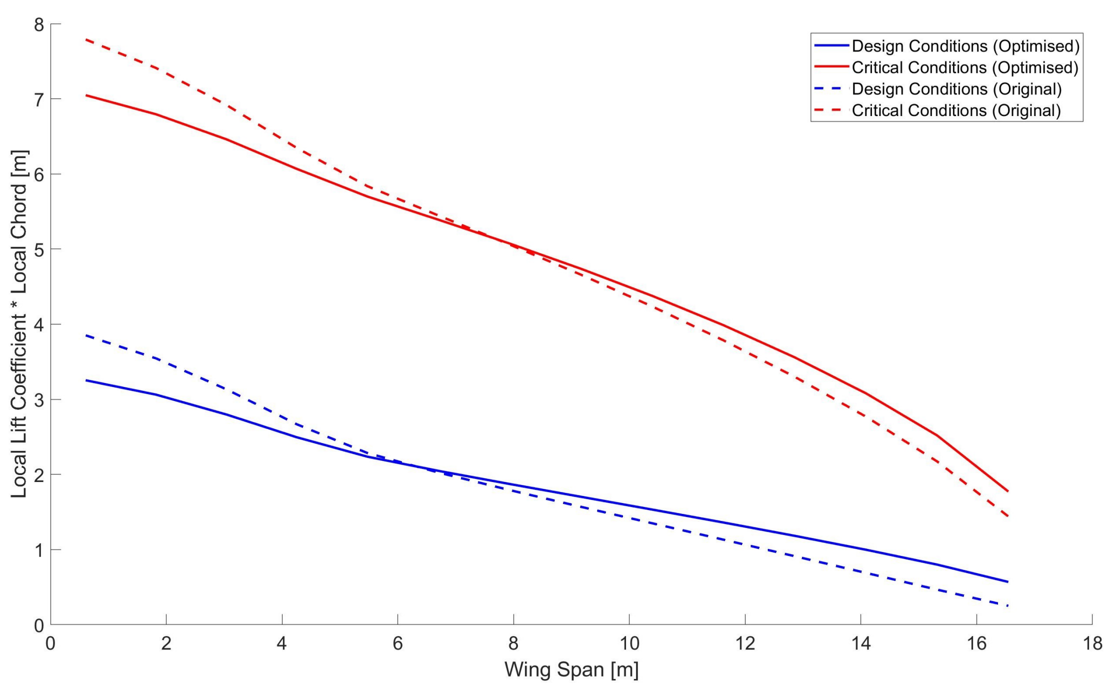

Figure 5: Spanwise lift distribution at design conditions (load factor = 1, W_{des} = 532981N [initial] & 533102N [optimized], v_{cruise} = 231.5 m/s, M_{cruise} = 0.7846, h_{cruise} = 11887.2m) and critical conditions (load factor = 2.5, $M_{TO,max}$ = 638537N [initial] & 627646N [optimized], v_{crit} = 247.86 m/s, M_{crit} = 0.84, h_{cruise} = 11887.2m)

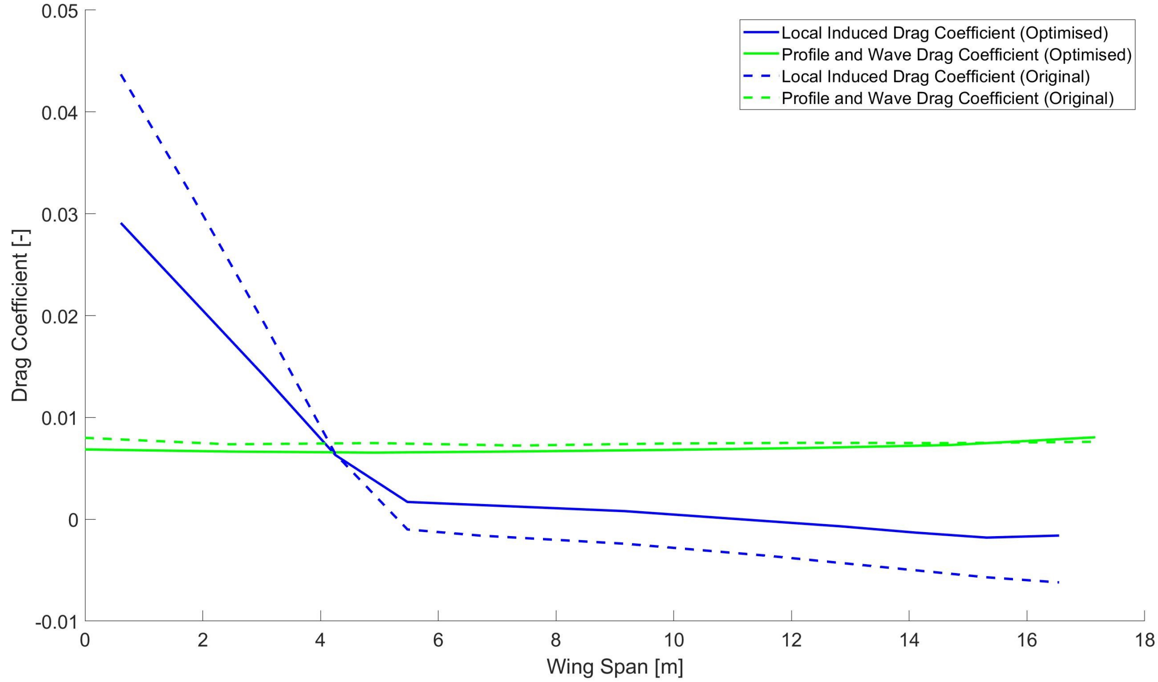

Figure 6: Spanwise drag coefficients at design point for initial and optimized wings (load factor = 1, W_{des} = 532981N [initial] & 533102N [optimized], v_{cruise} = 231.5 m/s, M_{cruise} = 0.7846, h_{cruise} = 11887.2m)

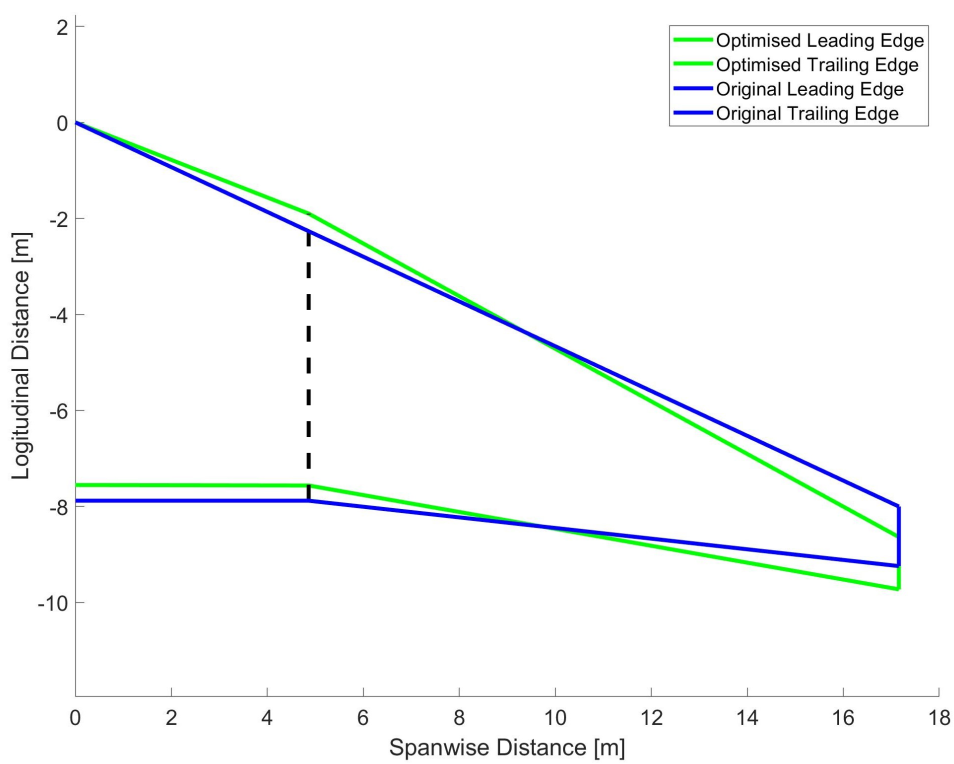

Figure 7: Initial and optimized wing planform viewed from above

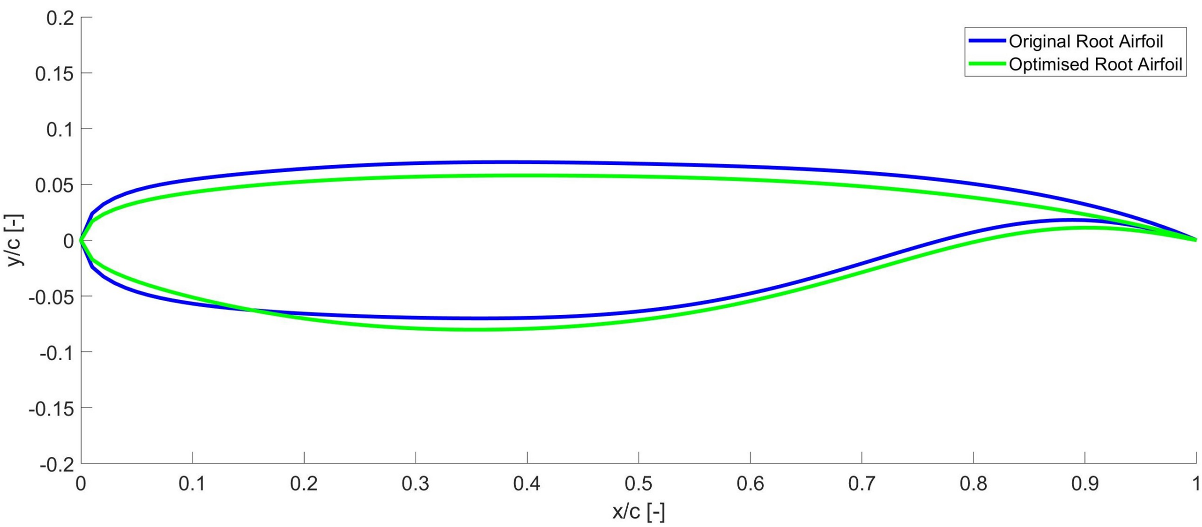

Figure 8: Initial and optimized root airfoil. Chord length = 1.

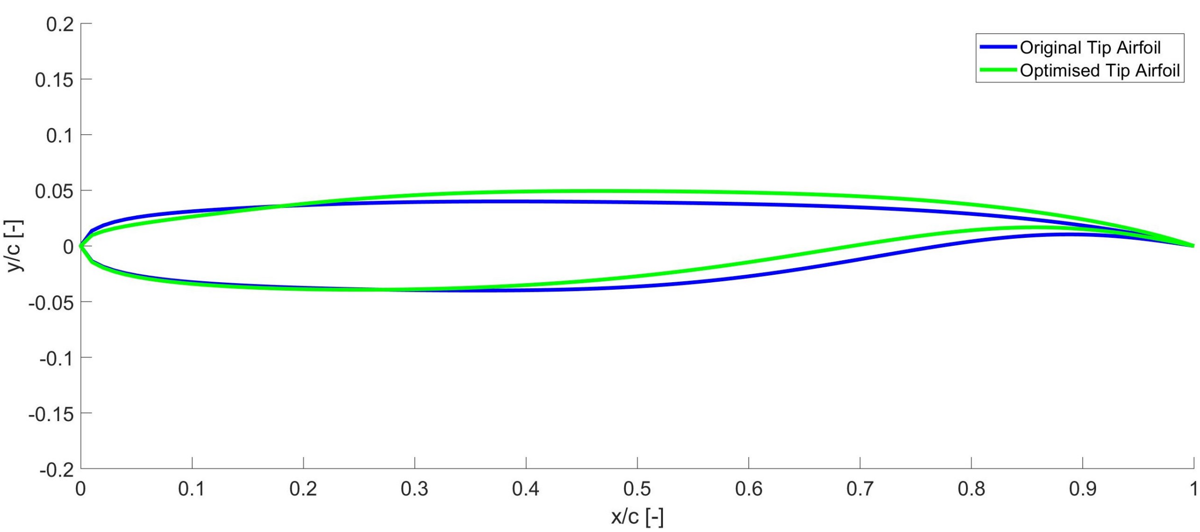

Figure 9: Initial and optimized tip airfoil. Chord length = 1.

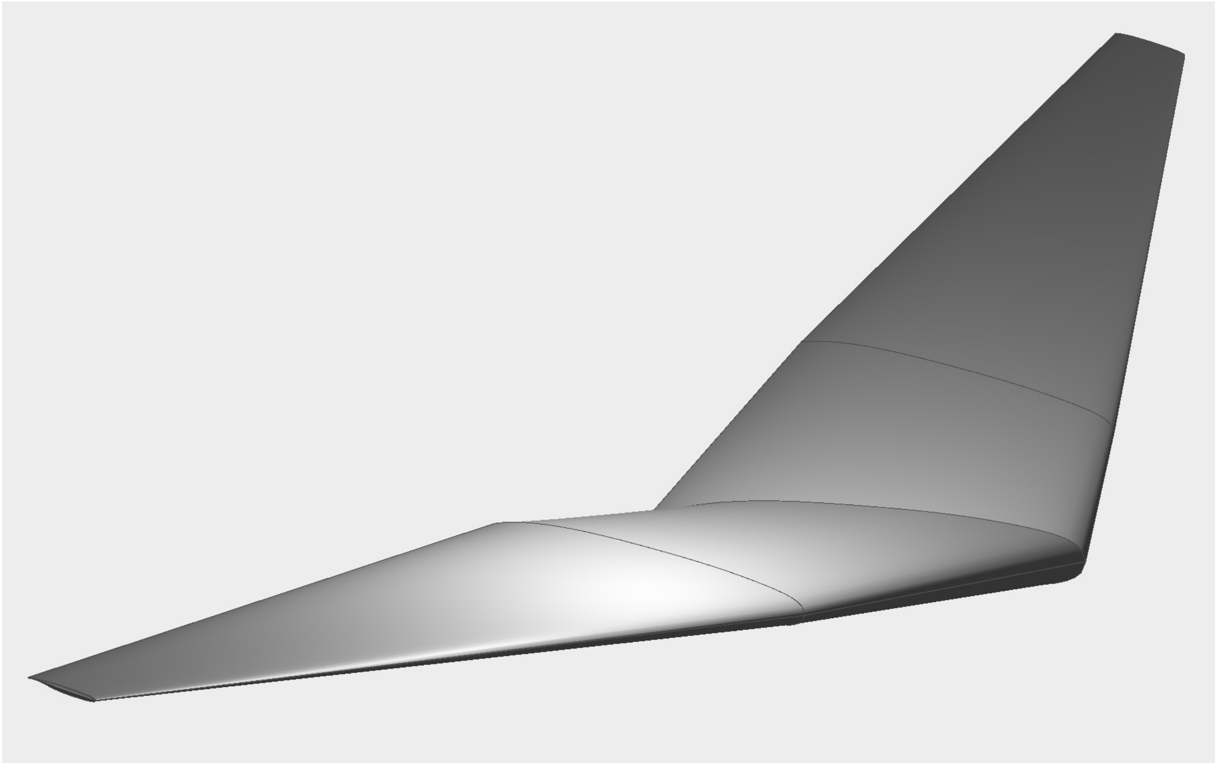

Figure 10: Isometric view initial wing

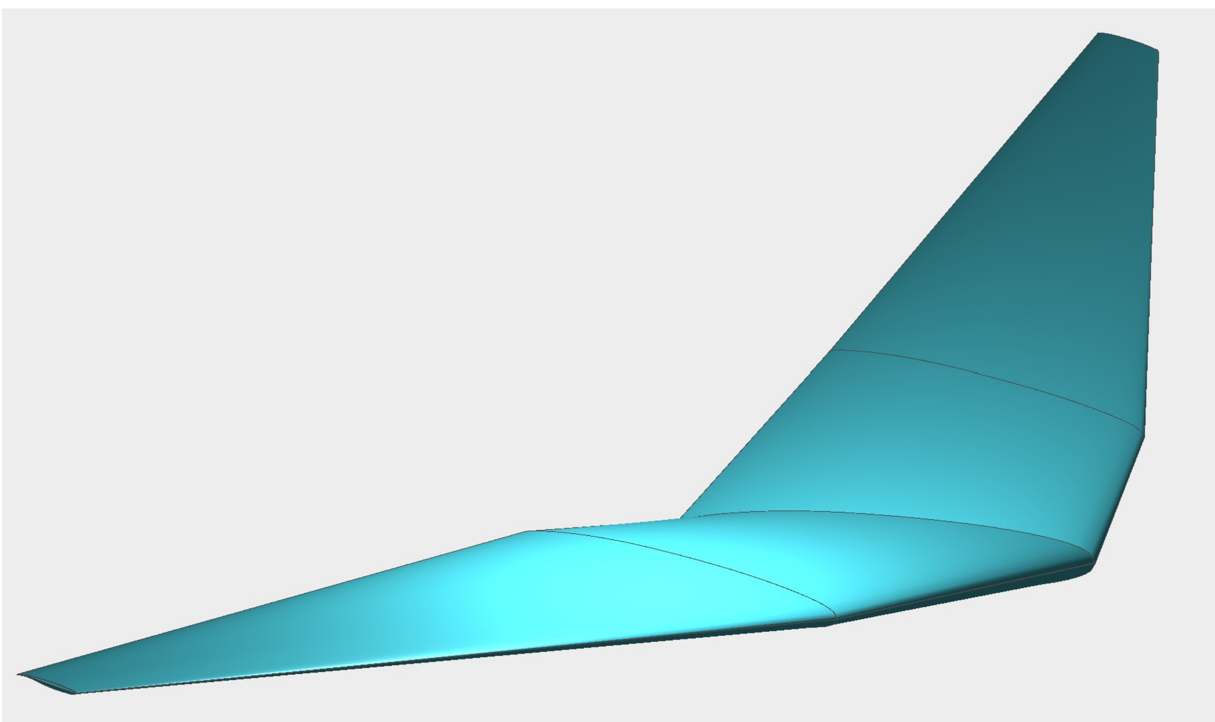

Figure 11: Isometric view optimized wing

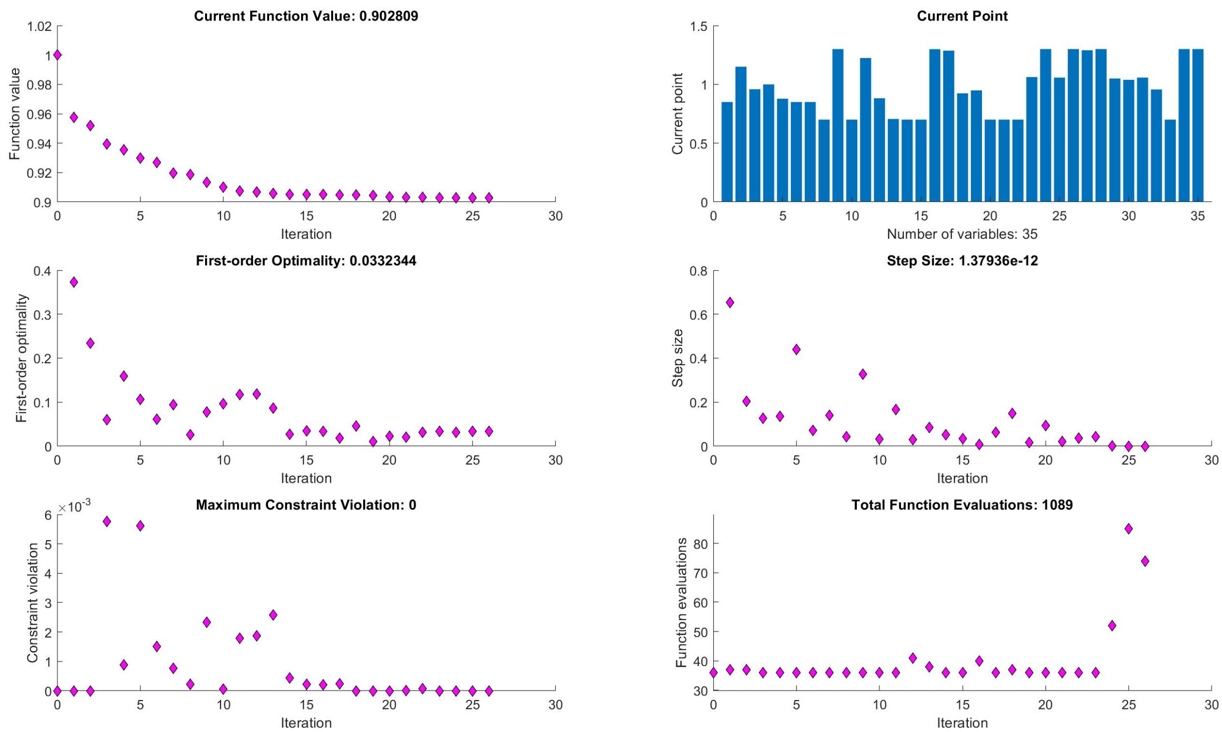

Figure 12: Matlab Optimisation Plots

3.4 Conclusions and critical reflection

3.4.1 Did the optimization converge to an optimum? How did you verify that?

The optimization might have reached a global optimum, but this cannot be verified 100% as the first-order optimality is non-zero. The first-order optimality is very low at 0.0332344, so it can be said with reasonable confidence that an optimum has been reached. The step size has reduced to less than 1e-12 and neither of the inequality constraints were violated. Therefore, the optimizer found the final design point to be of sufficient quality to terminate the run, which in the end led to a 9.72% reduction in the objective.

A manual way of verifying whether a local optimum has been reached would be to evaluate the Karush–Kuhn–Tucker (KKT) conditions for the design point, where if the constraints create an opposing gradient to the objective function with respect to all the design variables that have not reached their upper or lower bounds, then a local optimum has indeed been reached.

3.4.2 How did the optimization modify the initial design? Do these changes match your expectations and why (or why not)?

Figures 7, 8 and 9 show how the wing has changed geometrically. As covered in section 3.3, the optimizer tried to increase the aspect ratio by decreasing the chord lengths as the wing span could not be increased. The radius of the leading edge of the root airfoil decreased significantly, possibly hinting at an optimization of the chordwise isobar alignment. The total surface area of the wing did not change significantly as the maximum take-off weight barely changed (from 638537N to 627646N) and the wing loading constraint had to be met. Further, the relative wing span was increased by means of increasing the outer trapezoid leading edge sweep, further increasing the aspect ratio of the wing. All of these changes were expected. The biggest improvements in fuel consumption can be achieved by increasing the aspect ratio. The optimizer tried to do exactly this while simultaneously satisfying the wing loading constraint.

3.4.3 Are there any active constraints?

Figure 4 gives the impression that the wing loading constraint was active throughout most of the optimisation, and probably played an important part in the evolution of the design variable. However, the last three iterations showed no constraint violation, even though a constraint tolerance of 1e-6 was permitted (visible in Figure 12). Therefore, it is safe to say that there were no active constraints at the end of the optimisation.

3.4.4 What were the most influential design variables (and why)?

It seems that by only the second iteration, the objective had reduced a reasonable amount while not violating the constraints very drastically, and the geometric design variables responsible for this improvement seemed to be the inner sweep, kink twist and tip twist angles (as they had decreased to 85% their reference value already). From the airfoil side, it seems like the upper root airfoil coefficients were also very influential, as 4 out of the 7 had already reduced to their lower bound (70%).

3.4.5 Is your optimum point dictated by the bounds of your design variables?

Yes. Many of the values of the optimized design variable are at their lower or upper bounds. The twist angles are both at 85% of their original values. In hindsight, the twist angles could have been given more freedom all the way to values of perhaps -100% because they do not play an important role in the inconsistency constraints while they do affect the local angle of attack. A higher local angle of attack increases the lift coefficient which in turn improves aerodynamic performance.

The chord lengths, though the optimizer wanted to reduce them to increase the aspect ratio, had to stay relatively close to 1 to keep the surface area relatively similar to the original wing surface area.

Some of the Bernstein coefficients stayed close to 1 as well, because a drastic change in consecutive Bernstein coefficients (for e.g., 1.3 to 0.7) may lead to aerodynamically unfeasible airfoils (ones that Q3D may not be able to analyse) and therefore, aerodynamically invalid results.